Critical behavior of a three-dimensional hardcore-cylinder composite system

Jaime Silva,[1,2] Ricardo Simoes,[2,3] and Senentxu Lanceros-Mendez[1,*]
[1]*Center of Physics, University of Minho, Campus de Gualtar, 4710-057 Braga, Portugal*
[2]*Institute for Polymers and Composites IPC/I3N, University of Minho, Campus de Azurém, 4800-058 Guimares, Portugal*
[3]*School of Technology, Polytechnic Institute of Cavado and Ave, 4750-810 Barcelos, Portugal*
(Received 22 October 2011; revised manuscript received 15 December 2011; published 9 February 2012)

In this work the critical indices β, γ, and ν for a three-dimensional (3D) hardcore cylinder composite system with short-range interaction have been obtained. In contrast to the 2D stick system and the 3D hardcore cylinder system, the determined critical exponents do not belong to the same universality class as the lattice percolation, although they obey the common hyperscaling relation for a 3D system. It is observed that the value of the correlation length exponent is compatible with the predictions of the mean field theory. It is also shown that, by using the Alexander-Orbach conjuncture, the relation between the conductivity and the correlation length critical exponents has a typical value for a 3D lattice system.

DOI: 10.1103/PhysRevE.85.021115 PACS number(s): 64.60.ah, 45.50.Jf, 64.60.aq

I. INTRODUCTION

The percolation problem of two-dimensional (2D) random sticks was first addressed by Pike and Seager [1], with the authors focusing on the determination of the point of emergence of the giant component that spans the system, i.e., the percolation threshold [2,3]. Later, Balberg *et al.* [4] derived the percolation critical exponents for the 2D random sticks problem, demonstrating that the 2D continuum percolation problem belongs to the same universality class as the lattice percolation; i.e., the continuum and the lattice percolation problems share the same critical exponents. The latter is in agreement with the expected universality of the critical exponents, as they depend just on the system dimension, the symmetry of the order parameter, and the range of interactions [5]. It was also established that the percolation threshold is proportional to the inverse of the expected excluded volume (3D) or area (2D) of the stick, i.e., the volume (area) around a object into which the center of another similar object is not allowed to enter [6–8]. With carbon nanotubes [9] and their wide application range [10], the percolation problem of 2D and 3D random rods becomes an essential framework to study the experimental results of the growing field of carbon nanotube and polymer composites. One of the first works comparing experimental results on polymers reinforced with carbon fibers with the theoretical predictions from the excluded volume theory and determining the bounds for the percolation threshold of high-aspect ratio rods was presented by Clelzard *et al.* [11]. This work was followed by studies related to the determination of the percolation threshold of 2D or 3D rod systems [12–19]. The relevance of these works for the material science field was recently summarized in a review article [20]. Remarkably, while for the 2D softcore problem the determination of the critical exponents has been reported [4], few studies [21–23] are focused on the determination of the critical exponents for 3D hardcore caped cylinders with an isotropic distribution. In fact, in the works of Dani and Ogale [22,23] and Ogale and Wang [21] the system has some degree of anisotropy in order to better model the composite processing conditions and the hardcore fillers have a low aspect ratio. In this way, Dani and Ogale [22,23] calculated the γ, σ, τ, and ν critical exponents and the fractal dimension of the 3D continuum short-fiber composite. It was found that the values of the critical exponents are in agreement with the values for the 2D and 3D lattice systems and 2D continuum systems reported in the literature. The correlation length critical exponent was also calculated [21] and it was found that it is in agreement with the values for 3D lattice systems. A recent experimental study for carbon nanofiber and polyimide composites [24] determined the critical geometrical exponent, β, reporting that it belongs to the same universality class of a Bethe lattice, i.e, $\beta = 1$. This experimental result has been theoretically explained [25] through the application of the network theory to carbon nanofiber nanocomposites, by mapping fillers to vertices and edges to the gap between fillers.

In this work, the critical behavior for composites filled with high-aspect ratio cylinders interacting with each other by a short-range potential is analyzed. The critical exponents β, γ, and ν are calculated using a finite size scaling analysis [2] with the objective of clarifying previous studies on the dimension of the clusters criticality for an isotropic system with hardcore fillers with a high-aspect ratio.

II. SIMULATION PROCEDURE

The microstructure for the isotropic materials is generated by a derivation of a sequential packing algorithm [26] to place randomly oriented cylinders in 3D space and using periodic boundary conditions; i.e, when part of a cylinder crosses the domain boundary it is cut and the segment that crosses the boundary is translated to the opposite domain boundary (i.e., symmetrically translated). After creating the virtual composite, the graph theory framework is used to study the composite's percolation threshold. Within this framework, the cylinders are mapped to vertices and the edges to the minimum distance between the cylinders, which corresponds to the maximum electric field between the two fillers [27]. A maximum value for the minimum separation distance $\delta_{\max}$ is defined [27] and an undirected graph is constructed from the generated microstructure. The edges (junction between cylinders) of the graph are assigned if the minimum separation

*lanceros@fisica.uminho.pt

distance is less than δ_{max}. The generated microstructure corresponds to a cube with side L and five different cube side lengths were simulated, $L = 300$, 400, 500, 600, and 700. Cubes were filled with cylinders with aspect ratios of 100 and $\delta_{max} = 1$ and the generated volume fractions ranged from 10^{-4} to 4.1×10^{-3}, corresponding to a number of cylinders from a few hundred to $\sim 10^4$. It is stressed that by increasing the δ_{max} value the number of connected cylinders is increased, shifting the percolation threshold to lower values.

For each data point (set of material parameters) of the results shown, $\sim 10^4$ different microstructures were simulated and all the respective graph properties were averaged. More precisely, using a breadth-first search algorithm [28] the size of the largest component, giant component S, was calculated by monitoring the size distribution, $P(s)$, of finite clusters, excluding the size of the largest cluster, to which a random node belongs, $P(s) = sn(s)/s_{av}$. Here, s is the number of vertices, $n(s)$ is the cluster size distribution, and s_{av} is the ratio of the number of vertices to the total number of clusters. By knowing $P(s)$, the size of the giant component can be calculated, $S = 1 - \sum_s P(s)$, as well as the mean size of a finite cluster to which a random vertex belongs, $\langle s \rangle = \sum_s s P(s)$.

III. RESULTS AND DISCUSSION

In Fig. 1(a) the evolution of the size of the giant component, S, as a function of the volume fraction for different domains sizes is presented. Figure 1(b) shows the mean size of the finite clusters, $\langle s \rangle$, as a function of the cylinder volume fraction. Also in Fig. 1(b) it is observed that the maximum value of $\langle s \rangle$ increases with increasing system size and it is possible to extrapolate that, when $L \to \infty$, $\langle s \rangle \to \infty$ at the percolation threshold. In the system under study the size of the giant component, S, takes the role of the order parameter and the mean size of the finite clusters, $\langle s \rangle$, takes the role of the susceptibility [29]. It is observed in Fig. 1 that the order parameter changes continuously and the susceptibility diverges at the percolation threshold. The order parameter takes the value of zero in the most symmetric phase and nonzero in the least symmetric phase; e.g., there is a symmetry break or change at the phase transition. If the order parameter changes continuously at the percolation threshold and there is a divergence in the susceptibility, the transition is termed

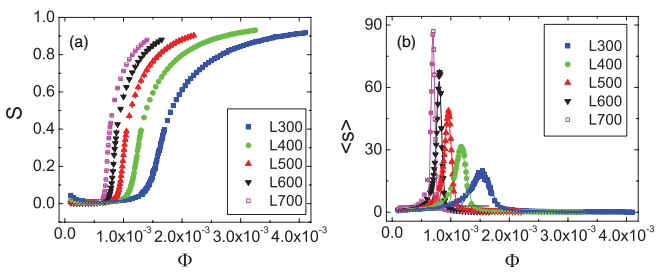

FIG. 1. (Color online) (a) Size of the giant component as a function of the volume fraction. (b) Size of the finite cluster, excluding the giant component, as a function of the volume fraction. Results have been averaged over $\sim 10^4$ samples. Error bars are smaller than the data points.

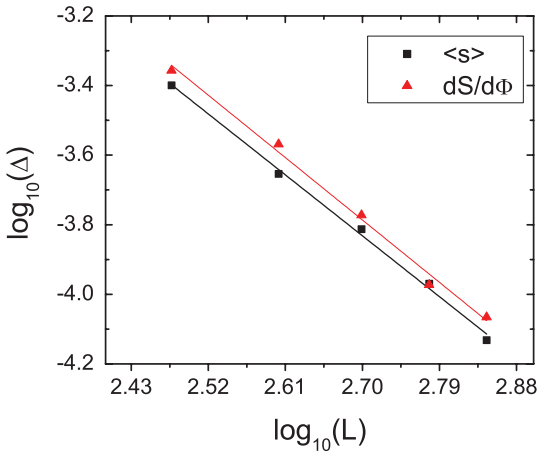

FIG. 2. (Color online) Width of the transition versus system dimension in a log-log plot. The lines are linear fits to the data.

second-order (Fig. 1). It is known [2] that for a second-order phase transition the width of the transition, Δ, should scale with the system size as $\Delta \sim L^{-\frac{1}{\nu}}$, where ν is related with the correlation length, ξ. The width of the transition can be naturally calculated by fitting $\langle s \rangle$ to a Gaussian and using the full width at half maximum (FWHM) of the Gaussian as the value for Δ. Another approximation [2] is using a Gaussian to fit $\frac{dS}{d\phi}$ as a function of ϕ and taking the value of the Gaussian FWHM as the value for Δ. The two methods, previously described, were employed in the determination of Δ and the results are summarized in Fig. 2. In Fig. 2, one can observe that in a log-log scale there is a linear relationship between the width of the transition, Δ, and the length of the domain, L. As can be observed in Fig. 2 the two methods give similar results. More precisely, the calculated correlation length critical exponents are $\nu = 0.502 \pm 0.022$ for the method based on the order parameter and $\nu = 0.514 \pm 0.016$ for the method based on the susceptibility. The latter values lead to the conclusion that ν is compatible with the mean field value, i.e., $\nu = 1/2$. Once the value for the correlation length exponent is obtained, it is possible to determine other critical exponents using a finite size scaling analysis (FSS) [2]. It should be pointed out that FSS analyses have already been successfully applied to networks [30]. In this work we use the volume fraction, ϕ, as the control parameter instead of the number of vertices due to the fact that the former can be easily related to experimental works. As the two parameters are related by a linear relation it is expect that the obtained critical exponents will be the same. Close to the critical volume fraction, the correlation length, ξ, is comparable to the system size and therefore the size of the giant cluster, S, should scale as

$$S = L^{-\frac{\beta}{\nu}} F\left[L^{\frac{1}{\nu}}(\phi - \phi_c)\right], \tag{1}$$

where F is a suitable scaling function. The FSS also predicts that $\langle s \rangle$ should scale with the system size, L, as

$$\langle s \rangle = L^{\frac{\gamma}{\nu}} F_1\left[L^{\frac{1}{\nu}}(\phi - \phi_c)\right], \tag{2}$$

where the scaling function, F_1, in Eq. (2) is different from the one in Eq. (1). The latter equations are expected to scale at $\phi = \phi_c$ as power laws. Using the ϕ_c and the height of the Gaussian fits to $\langle s \rangle$, presented in Fig. 1(b), it is possible to use

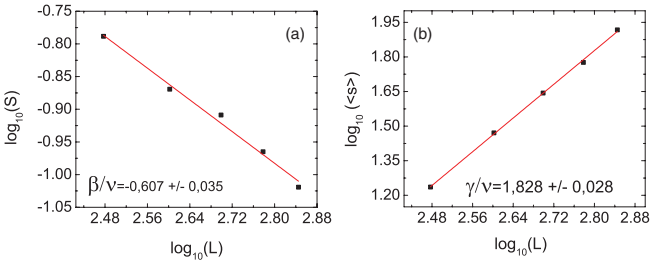

FIG. 3. (Color online) (a) Double logarithm plot of the size of the giant component, at ϕ_c, for the different domain sizes, L. (b) Double logarithm plot of the height of the fitted Gaussian for the different domain sizes, L.

the latter scaling relations to obtain the critical exponents. For the determination of $\frac{\beta}{\nu}$, the size of the giant component at ϕ_c for the different domain sizes was used, as presented in Fig. 3(a) in a double logarithm scale. To establish the value of $\frac{\gamma}{\nu}$, the height of the fitted Gaussian for the different domains sizes was plotted in a double logarithm scale as shown in Fig. 3(b). The linear relations that are obtained in Fig. 3, $R^2 \sim 0.99$ for the two fits, demonstrate that the two scaling laws, Eqs. (1) and (2), are obeyed. The FSS theory also predicts that near ϕ_c the curves for the different domain sizes should collapse in one curve. It is possible to observe this fact in Fig. 4(a) for the order parameter and in Fig. 4(b) for the susceptibility. Using the obtained values for ν it is possible to determine β and γ. So, $\beta = 0.305 \pm 0.022$ using $\nu = 0.502 \pm 0.022$ and $\beta = 0.312 \pm 0.020$ using $\nu = 0.514 \pm 0.016$. The obtained values for γ are $\gamma = 0.918 \pm 0.043$ using $\nu = 0.502 \pm 0.022$ and $\gamma = 0.940 \pm 0.033$ using $\nu = 0.514 \pm 0.016$, which are close to the mean field value, $\gamma = 1.0$. Interestingly, it is known that the hyperscaling relation [2,3]

$$d = 2\frac{\beta}{\nu} + \frac{\gamma}{\nu} \tag{3}$$

should be obeyed up to the critical dimension, $d_c \leqslant 6$. Using Eq. (3) with the critical exponents calculated from the data presented in Fig. 3, then $d = 3.041 \pm 0.075$, which is in accordance with the 3D system. The reported critical exponents do not agree with the critical exponents for the 3D lattice universality class [2,3], i.e, $\beta_{3D} = 0.4$, $\gamma_{3D} = 1.8$, and $\nu_{3D} = 0.9$. As the latter exponents are not exact values we round them to the first decimal place. On the other hand, our calculated values for β and ν have been found in experimental work [31] related to the critical behavior of a phase transition in the near surface region. Interestingly, another model that

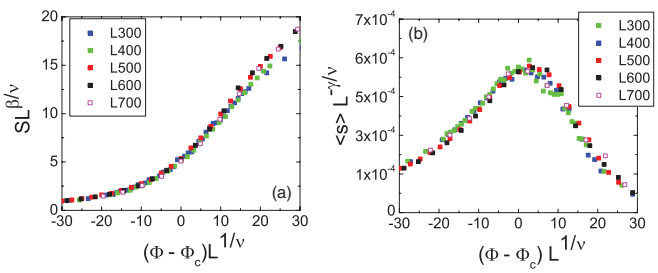

FIG. 4. (Color online) (a) $SL^{\frac{\beta}{\nu}}$ vs $(\Phi - \Phi_c)L^{\frac{1}{\nu}}$. (b) $\langle s \rangle L^{-\frac{\gamma}{\nu}}$ vs $(\Phi - \Phi_c)L^{\frac{1}{\nu}}$.

exhibits a tricritical point and shares the same critical exponent, $\beta = 0.3$, was recently proposed by Cellai *et al.* [32] in the context of the k-core percolation. The values of the obtained critical exponents can be used to calculate the conductivity critical exponent which is known to follow a power law: $\sigma \sim (\phi - \phi_c)^t$, where σ is the system conductivity. For a 3D system and using the previous critical exponents [2]:

$$\frac{t}{\nu} \sim 2.2. \tag{4}$$

The obtained value of Eq. (4) can be also deduced by the determined critical exponents using the Alexander-Orbach conjuncture [33]. The Alexander-Orbach conjuncture is based on the diffusion on fractals and predicts that the dimensionality of the quantized vibrational states on a fractal is close to $\frac{4}{3}$ for $d \geqslant 2$, independent of the system dimensionality. The latter implies that

$$\frac{t}{\nu} = \frac{1}{2}(3d - 4) - \frac{\beta}{2\nu}. \tag{5}$$

Solving Eq. (5) for a 3D system and with the calculated $\frac{\beta}{\nu}$ from Fig. 3 results in $\frac{t}{\nu} = 2.197 \pm 0.018$, which is in accordance with Eq. (4), within the determined error, for a 3D system. In particular the t has a value of 1.103 ± 0.049 using $\nu = 0.502 \pm 0.022$ and of 1.129 ± 0.036 using $\nu = 0.514 \pm 0.016$. The latter values are close to the one, 1.0, obtained by the effective medium theory [34].

IV. CONCLUSION

In conclusion, the critical exponents for a hardcore 3D cylinder system with short-range interactions has been obtained, making use of the network theory, and these are related through the common hyperscaling for a 3D system. In contrast to the 2D stick system and the 3D hardcore cylinder system, the determined critical exponents do not belong to the same universality class as the lattice percolation. Instead, the correlation length critical exponent has a typical mean field value, the γ critical exponent has a value that is close to the mean field one, and $\beta = 0.3$. Interestingly, using the Alexander-Orbach conjuncture, it is found that the relation between the conductivity and the correlation length critical exponents for a 3D system is obeyed.

ACKNOWLEDGMENTS

The authors are in debt to Alberto Proença for providing the computational resources (SEARCH) used in this work. J.S. thanks Davide Cellai for a stimulating discussion. The numerical calculations were performed on the Advanced Research Computing Services with HTC/HPC clusters and the SEARCH cluster, financed through the Programa de Reequipamento Científico Nacional, FCT-Fundação para a Ciência e a Tecnologia, CONC-REEQ/443/EEI/2005, and by the Program POCI 2010 funded by FEDER. This work is also funded by FEDER funds through the "Programa Operacional Factores de Competitividade COMPETE" and by the FCT: Project References PTDC/CTM/69316/2006, NANO/NMed-SD/0156/2007, PTDC/EME-PME/108859-2008, and

PTDC/CTM-NAN/112574/2009. J.S. is financed through FCT Grant No. SFRH/BD/60623/2009. The authors also acknowledge support from COST Action MP1003 (European Scientific Network for Artificial Muscles) and COST Action MP0902 [Composites of Inorganic Nanotubes and Polymers (COINAPO)].

[1] G. E. Pike and C. H. Seager, Phys. Rev. B **10**, 1421 (1974).
[2] D. Stauffer and A. Aharony, *Introduction to Percolation Theory* (Taylor & Francis, London, 1992).
[3] J. W. Essam, Rep. Prog. Phys. **43**, 53 (1980).
[4] I. Balberg, N. Binenbaum, and C. H. Anderson, Phys. Rev. Lett. **51**, 1605 (1983).
[5] R. B. Griffiths, Phys. Rev. Lett. **24**, 1479 (1970).
[6] I. Balberg, C. H. Anderson, S. Alexander, and N. Wagner, Phys. Rev. B **30**, 3933 (1984).
[7] I. Balberg, N. Binenbaum, and N. Wagner, Phys. Rev. Lett. **52**, 1465 (1984).
[8] A. L. R. Bug, S. A. Safran, and I. Webman, Phys. Rev. Lett. **54**, 1412 (1985).
[9] S. Iijima, Nature (London) **354**, 56 (1991).
[10] R. H. Baughman, A. A. Zakhidov, and W. A. de Heer, Science **297**, 787 (2002).
[11] A. Celzard, E. McRae, C. Deleuze, M. Dufort, G. Furdin, and J. F. Marêché, Phys. Rev. B **53**, 6209 (1996).
[12] S. H. Munson-McGee, Phys. Rev. B **43**, 3331 (1991).
[13] M. Foygel, R. D. Morris, D. Anez, S. French, and V. L. Sobolev, Phys. Rev. B **71**, 104201 (2005).
[14] L. Berhan and A. M. Sastry, Phys. Rev. E **75**, 041121 (2007).
[15] L. Berhan and A. M. Sastry, Phys. Rev. E **75**, 041120 (2007).
[16] P. van Der Schoot and A. V. Kyrylyuk, Proc. Natl. Acad. Sci. USA **105**, 8221 (2008).
[17] A. P. Chatterjee, J. Phys. Condens. Matter **20**, 255250 (2008).
[18] R. H. J. Otten and P. van der Schoot, Phys. Rev. Lett. **103**, 225704 (2009).
[19] A. P. Chatterjee, J. Chem. Phys. **132**, 224905 (2010).
[20] C.-W. Nan, Y. Shen, and J. Ma, Annu. Rev. Mater. Res. **40**, 131 (2010).
[21] A. A. Ogale and S. F. Wang, Combust. Sci. Technol. **46**, 379 (1993).
[22] A. Dani and A. A. Ogale, Combust. Sci. Technol. **56**, 911 (1996).
[23] A. Dani and A. A. Ogale, Combust. Sci. Technol. **57**, 1355 (1997).
[24] A. Trionfi, D. H. Wang, J. D. Jacobs, L. S. Tan, R. A. Vaia, and J. W. P. Hsu, Phys. Rev. Lett. **102**, 116601 (2009).
[25] J. Silva, R. Simoes, S. Lanceros-Mendez, and R. Vaia, Europhys. Lett. **93**, 37005 (2011).
[26] M. J. Vold, J. Phys. Chem. **63**, 1608 (1959).
[27] R. Simoes, J. Silva, R. Vaia, V. Sencadas, P. Costa, J. Gomes, and S. Lanceros-Mendez, Nanotechnology **20**, 35703 (2009).
[28] T. H. Cormen, C. E. Leiserson, R. L. Rivest, and C. Stein, *Introduction to Algorithms* (MIT Press, Cambridge, MA, 2001).
[29] M. E. J. Newman, SIAM Rev. **45**, 167 (2003).
[30] H. Hong, M. Ha, and H. Park, Phys. Rev. Lett. **98**, 258701 (2007).
[31] B. Burandt, W. Press, and S. Haussuhl, Phys. Rev. Lett. **71**, 1188 (1993).
[32] D. Cellai, A. Lawlor, K. A. Dawson, and J. P. Gleeson, Phys. Rev. Lett. **107**, 175703 (2011).
[33] S. Alexander and R. Orbach, J. Phys. Lett. **43**, 625 (1982).
[34] S. Kirkpatrick, Rev. Mod. Phys. **45**, 574 (1973).